Letters

Parameter Identification of the Series Inductance in DAB Converters

Zhiqiang Guo, *Member, IEEE*, Yong Luo, and Kai Sun, *Senior Member, IEEE*

***Abstract*—This letter presents a parameter identification of the series inductance in dual active converter. In the optimized modulation strategies and feedforward control, the series inductance is a key parameter to determine the performance of the converter. The series inductance is varied with many factors, such as the temperature, air gap, and switching frequency. The deviation value of the series inductance will cause the failure of the control strategy. In this letter, a parameter identification method is presented based on the recursive least squares algorithm. By using this method, the real value of the series inductance is derived. Finally, the effectiveness of the identification method is verified by the feedforward control in dual active bridge converters. The feedforward control can achieve good dynamic response by using the identification method, even if the real series inductance value is unknown.**

***Index Terms*—Dual active bridge (DAB), feedforward, parameter identification.**

I. Introduction

DUAL active bridge (DAB) converter is a prevalent solution in energy storage system [1], [2]. The galvanic isolation and soft switching can interface the different voltage levels for high-efficiency power conversion.

Linking the two full bridges with a transformer and a series inductor, the DAB converter can be controlled by using phase shift modulation. In order to achieve high efficiency in wide voltage conversion ratio, dual phase shift (DPS), enhanced phase shift (EPS), and triple phase shift (TPS) modulation schemes are proposed [3]–[5] to optimize the current stress and soft switching. To achieve soft switching and global minimum conduction loss, a modulation scheme combining different optimized working modes is proposed, and the working modes can achieve seamless transitions [6]. However, the minimum conduction loss in light load is associated with the series inductance. The deviation of the series inductance will cause more conduction loss or lose the zero-voltage switching.

A feedforward control is an effective solution to improve the dynamic response of the DAB converters. In [7], a phase estimator is developed as a feedforward path by using input and output power. Another feedforward compensation is proposed by first-order dynamic model of the DAB converter [8]. The lookup table should be calculated offline and stored in the microprocessor, which is an approximate solution. A virtual direct power control with feedforward control is developed for fast dynamic response [9], [10]. The feedforward path is designed on basis of the input and output power balance. A current sensorless control strategy with a disturbance observer is proposed to estimate the load current to improve the dynamic response [11]. To simplify the control strategy, a feedforward control is presented to reduce the computational complexity [12]. It is suitable for the low-cost digital controller. All above control strategies for DAB converters is on the premise that the series inductance is known in advance. However, the value of the inductance is associated with the flux density, which is very sensitive with many factors, such as the temperature, air gap, and switching frequency. If the ambient factors are changed, the value of the series inductance will be also changed. Therefore, the uncertainty of the series inductance will degrade the performance of the forementioned optimized modulation scheme and feedforward control. A deadbeat current control is proposed to achieve good dynamic response [13]. The current in the transformer can track the current reference in one switching cycle. However, the current in the series inductor at the specific time in each switching period should be sampled. Therefore, high bandwidth current sensor and high precious AD converter should be used. The sample delay may cause failure of the control strategy. The accuracy of the series inductance is associated with the converges of the control strategy. An online autotuning method is proposed to estimate the series inductance. The estimate method is also based on the high accuracy of the current sample.

In this letter, an identification of the series inductance in dual active converter is proposed to improve the feedforward control. The real value of the series inductance is identified in real time by using recursive least squares algorithm. The uncertainty of the series inductance is eliminated, so the dynamic performance of the DAB converter is improved. The rest of this letter is organized as follows. In Section II, the feedforward control in DAB converters is reviewed. Section III presents the parameter

Manuscript received November 5, 2020; revised December 1, 2020; accepted December 10, 2020. Date of publication December 21, 2020; date of current version March 5, 2021. This work was supported in part by the National Natural Science Foundation of China under Grant 51807007 and in part by the National Natural Science Foundation of China under Grant 51877117. *(Corresponding author: Zhiqiang Guo.)*

Zhiqiang Guo and Yong Luo are with the School of Automation, Beijing Institute of Technology, Beijing 100081, P.R. China (e-mail: guozq32@bit.edu.cn; 3120190915@bit.edu.cn).

Kai Sun is with the State Key Lab of Power Systems, Tsinghua University, Beijing 100084, P.R. China (e-mail: sun-kai@mail.tsinghua.edu.cn).

Color versions of one or more figures in this article are available at https://doi.org/10.1109/TPEL.2020.3045931.

Digital Object Identifier 10.1109/TPEL.2020.3045931

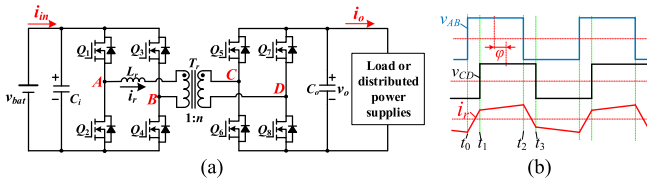

Fig. 1. Key waveforms of SPS control for DAB converters.

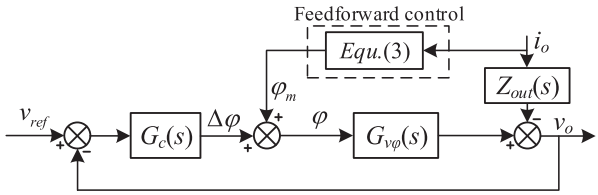

Fig. 2. Control diagram with feed-forward for DAB converter.

identification method. In Section IV, the experimental results are shown to verify the effectiveness of method. The dynamic response caused by the uncertainty of the series inductance is improved. Finally, the conclusion is given in Section V.

II. Review of the Feedforward Control Strategy in DAB Converters

Fig. 1 shows the circuit and key waveforms of SPS control for DAB converters, which is still the prevalent control scheme of DAB converter especially for high power application. In SPS control, v_{AB} and v_{CD} are square waveforms, and φ is the phase shift angle between v_{AB} and v_{CD}. L_r is the series inductance, T_s is the switching frequency, n is the turns ratio of the transformer, $v_{\rm bat}$ is the voltage of the battery, and v_o is the output voltage, which can link to the load or distributed power supply. The energy storage system can compensate the power mismatch of the distributed power supply and load. In this working mode, the dc-link voltage must be controlled by the energy storage system. DAB converters work in the dc-link control. The output power of the DAB converter in SPS control can be expressed as follows:

$$p_o = \frac{v_o v_{\rm bat} T_s}{8nL_r}\left(\frac{4\varphi}{\pi} - \frac{4\varphi^2}{\pi^2}\right). \tag{1}$$

In steady state, the load current in SPS control can be expressed as follows:

$$i_{\rm o} = \frac{p_o}{v_o} = \begin{cases} \frac{v_{\rm bat}T_s}{8nL_r}\left(\frac{4\varphi}{\pi} - \frac{4\varphi^2}{\pi^2}\right) i_o \geq 0 \\ \frac{v_{\rm bat}T_s}{8nL_r}\left(\frac{4\varphi}{\pi} + \frac{4\varphi^2}{\pi^2}\right) i_{\rm o} < 0. \end{cases} \tag{2}$$

As seen, the load current in steady state is independent of the output voltage. In steady state, the phase shift angle can be derived from the load current. The transient response of a single voltage loop is slow, because the phase shift angle is regulated by the output voltage error. At the load step change, the output voltage error is very low, so the phase shift angle is not regulated immediately. However, the load current is varied with the load at the dynamic process. According to (2), the desired phase shift angle can be calculated by the load current during the load variation, as seen in the following equation:

$$\varphi_m = \begin{cases} \frac{\pi}{2}\left(1 - \sqrt{1 - \frac{i_o}{I_{\rm base}}}\right) i_o \geq 0 \\ \frac{\pi}{2}\left(-1 + \sqrt{1 + \frac{i_o}{I_{\rm base}}}\right) i_o < 0 \end{cases} \tag{3}$$

where $I_{\rm base} = \frac{v_{\rm bat}T_s}{8nL_r}$.The load current can be sampled as the feedforward value in the closed-loop control. The control diagram with feedforward control is shown in Fig. 2. $Z_{\rm out}(s)$ is the output impedance, $G_{v\varphi}(s)$ is the transfer function of the control-to-output-voltage, and $G_c(s)$ is the output voltage controller. As seen in (3), i_o and $v_{\rm bat}$ can be sampled in a switching period, and T_s is the preset value. The output impedance and feedforward paths can be viewed as the disturbance of the closed-loop control, which is not associated with the stability of the control loop. Therefore, $G_c(s)$ can be designed as a DAB converter without feedforward control. According to (3), the gain of the feedforward path is based on the load current instead of a constant value. The gain of the feedforward path is adjusted dynamically with the load current. The turns ratio of the transformer depends only on the number of turns. The series inductance is uncertain in the control loop, which is sensitive to the temperature, air gap and the switching frequency. How to get the value of the series inductor in real time is the key issue of the feedforward control.

III. Identification of the Series Inductor in DAB Converter

Taking forward power flow for example, in steady state, the following equation can be derived from (2):

$$I_{\rm o} = \frac{V_{\rm bat}T_s}{8nL_r}\left(\frac{4\Phi}{\pi} - \frac{4\Phi^2}{\pi^2}\right) \tag{4}$$

where the capital letters are the corresponding quiescent values. Equation (4) is rewritten to obtain the following equation:

$$\left[1 - \left(1 - \frac{2\Phi}{\pi}\right)^2\right] T_s = \left(\frac{8nI_o}{V_{\rm bat}}\right) L_r. \tag{5}$$

In steady state, the phase shift angle and sampled values meet the following constraint:

$$\left[1 - \left(1 - \frac{2\Phi(k)}{\pi}\right)^2\right] T_s = \left(\frac{8nI_o(k)}{V_{\rm bat}(k)}\right) L_r \tag{6}$$

where $\Phi(k)$ represents the steady-state value of the phase shift angle in the kth sampling period, $I_o(k)$ and $V_{\rm bat}(k)$ are the kth sampled value in the steady state. Defining $y(k) = [1 - (1 - \frac{2\Phi(k)}{\pi})^2]T_s$ and $x(k) = \frac{8nI_o(k)}{V_{\rm bat}(k)}$, $y(k)$ is proportional to $x(k)$, and the scaling factor is the series inductance, $y(k)$ can be derived from the output of the controller, and $x(k)$ can be obtained from the sampled values. Therefore, L_r can be expressed as $L_r = \frac{y(k)}{x(k)}$.

There are noises in the sampled values, so the calculated series inductance also contains noises. Furthermore, the response of the identification method should be decoupled from the control loop. The recursive least squares (RLS) algorithm is an adaptive filter algorithm that recursively finds the coefficients that minimize a

weighted linear least squares cost function relating to the input signals. It can be used to identify the real-time value of the series inductance. The formula for recursive least squares is shown in the following equation:

$$\begin{aligned} e(k) &= y(k) - L_r(k-1)x(k) \\ K(k) &= \frac{P(k-1)x(k)}{\lambda + x(k)P(k-1)x(k)} \\ P(k) &= \frac{P(k-1)[1-K(k)x(k)]}{\lambda} \\ L_r(k) &= L_r(k-1) + K(k)e(k) \end{aligned} \tag{7}$$

where $L_r(k)$ is the kth value calculated by using the RLS algorithm. The forgetting factor λ is introduced to adjust the influence of old data, and $0 < \lambda < 1$. If λ is closer to 1, the result is more determined by the old data. If λ is closer to 0, the result is more determined by the new data. $P(k)$ and $K(k)$ are the intermediate variables. $P(0)$ is initially set as a very large value, where $P(0)$ is set as 10^6 in the experimental verifications. The derivation of the RLS algorithm is not the key issue in the article. The detailed formula of the RLS can be obtained from [14, Ch. 5].

The series inductance varies in very low frequency. The rate of converge for the identification method should be very low, but should incorporate new data. Therefore, λ is set large enough. In the experimental verifications, λ is set as 0.99. The identification method is in low-frequency response, and it is independent of control loop.

As seen in (6), when the load current is very low, especially for no load case, $y(k)$ and $x(k)$ are low values. In this case, they may be in the same magnitude with the sampling noise. Furthermore, the forward voltage and dead time of semiconductor devices will also cause error in light loads. The error caused by the deadtime of semiconductor devices can be compensated by adding a phase offset [13]. However, the voltage drop across the switches and the transformer winding resistance is hard to compensate in real time. Therefore, the identification method has large error in light loads. With the increase of the load power, the load current and φ become larger. Meanwhile, the uncertain factors mentioned above also become little impact on the identification method. When the load current is large enough, the identification method is implemented. In this letter, only when the load current is greater than 1.5 A, the algorithm is executed. Within the light load step change, the converter can achieve good dynamic performance even without the feedforward control. Therefore, the identification of the series inductance in light loads can be ignored.

Because SPS is the basic modulation scheme for DAB converter, it is taken as an example to explain this method. This identification method can also be extended to DPS, EPS, TPS, and other modulation schemes for DAB converters. Because the series inductance is varied in very low-frequency response. The RLS algorithm can be implemented once in a sampling period or serval sampling periods. As seen in (7), the algorithm contains seven multiplications, two additions, two subtractions, and two divisions. Testing in the digital signal processor (DSP) TMS320F28335 with 150 MHz clock frequency, the running time of the algorithm is proximately 550 ns at a time. Therefore, it is easily implemented in the DSP.

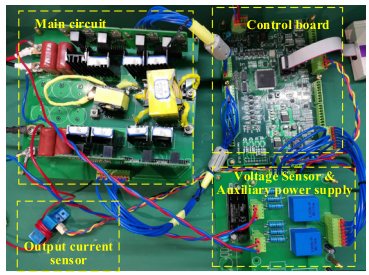

Fig. 3. Prototype for test.

TABLE I
DETAILED SPECIFICATIONS

Items	Symbol	Parameter
Battery voltage	V_{bat}	200 V
Output voltage	V_o	200 V
Turns ratio of the transformer	n	1
Switching frequency (period)	$f_s(T_s)$	50kHz (20 μs)
Switches	$Q_{1\text{-}8}$	FDA50N50 (FairChild)
Output filter capacitance	C_o	20μF

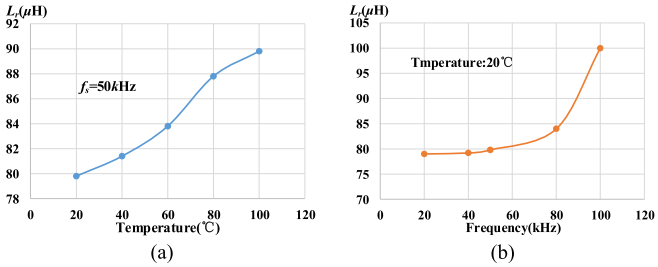

Fig. 4. Curves of the series inductance versus the temperature and frequency.

IV. EXPERIMENTAL VERIFICATION

A 1-kW prototype is built to verify the control strategy. Fig. 3 shows the prototype for test. The detailed specifications are shown in Table I. The control strategy is implemented in a TMS320F28335.

The series inductance including the leakage inductance of the transformer in the experimental prototype is tested by using an LCR meter in different temperatures and frequencies. The curves are shown in Fig. 4. Fig. 4(a) shows the curves of the series inductance versus the temperature in 50 kHz frequency. Fig. 4(b) shows the curves of the series inductance versus the frequency in 20 °C. The curves illustrate that the series inductance is varied with the temperature and frequency. Therefore, the performance of the feedforward control will be degraded when the ambient factors are changed.

All the following experimental results are tested in 20–30 °C room temperature. In 30 °C, the series inductance is proximate 81 μH. Fig. 5 shows the experimental results with feedward control for the load step change, when the series inductance is set as 81 μH. Before the load step change, the load power is

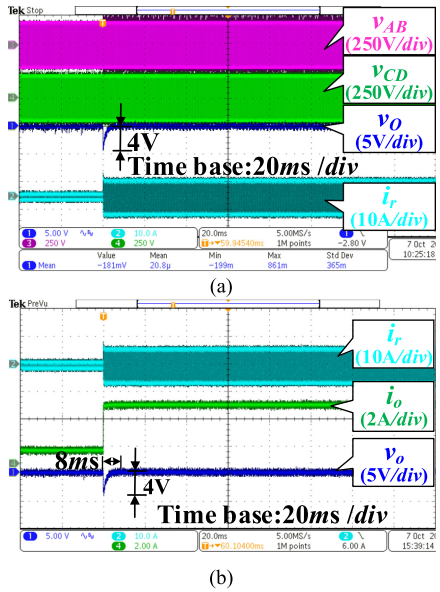

Fig. 5. Load step change with feedforward control when the series inductance is set as 81μH. (a) Voltage of the two full bridges, current in the transformer and output voltage. (b) Current in the transformer, output current, and output voltage.

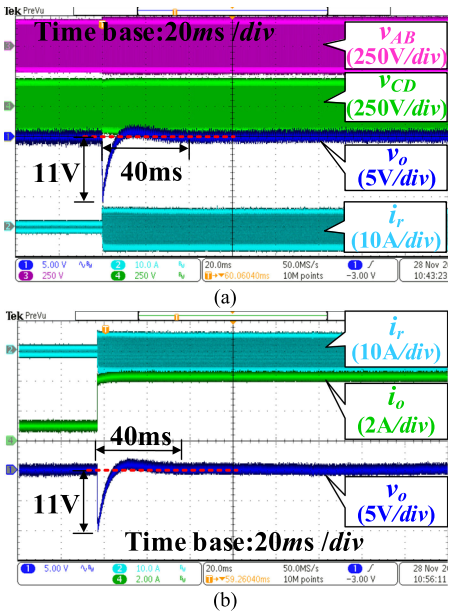

Fig. 6. Load step change when the series inductance is set as 70 μH. (a) Voltage of the two full bridges, current in the transformer, and output voltage. (b) Current in the transformer, output current, and output voltage.

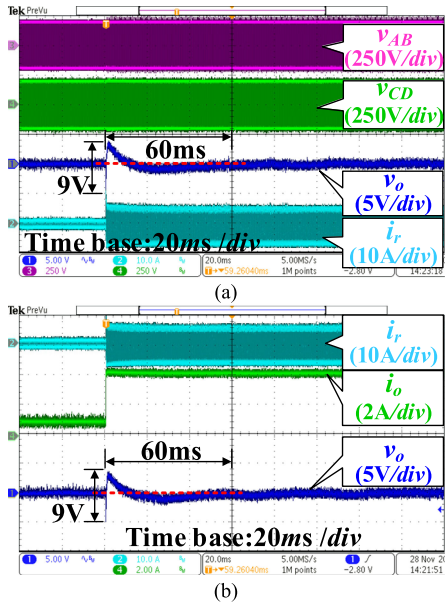

Fig. 7. Load step change when the series inductance is set as 90 μH. (a) Voltage of the two full bridges, current in the transformer and output voltage. (b) Current in the transformer, output current, and output voltage.

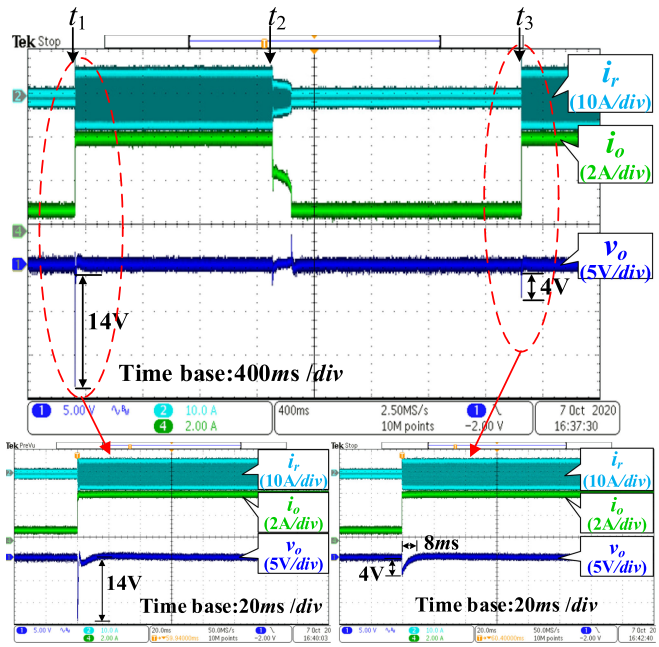

Fig. 8. Feedforward control with the identification of the series inductance.

200 W. The voltage drop is about 4 V and the settling time is 8 ms, when the load changes to 860 W. The converter can achieve good dynamic response with the feedforward control.

Fig. 6 shows the experimental results with feedforward control, when the value of the series inductance is set as 70 μH. The voltage drop reaches more than 11 V. Because the value of the series inductance in the control loop is less than the real value, the converter still has poor dynamic response.

Fig. 7 shows the experimental results with feedward control, when the series inductance is set as 90 μH in the feedforward control. The value of the series inductance in the control loop is greater than the real value, and it is with 10% of error. In this case, the voltage drop is overcompensated by the feedforward control. Although the voltage drop is very small, there are overshoot in the dynamic process. The voltage variation during the load step change reaches 9 V. The settling time is very large because of the overcompensated feedforward control.

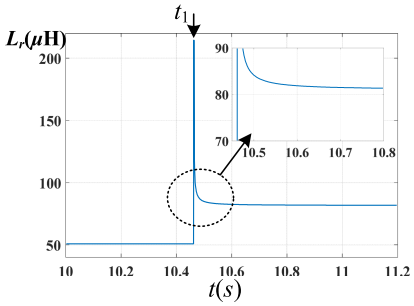

Fig. 9. Identification curve of the series inductance.

Fig. 8 shows the load step change by using feedforward control with the parameter identification of the series inductance. The value of the series inductance is initially set as 50 μH, which is less than the real value. During the startup, the load current is 1 A. It is very low, so the identification method is not implemented. At t_1, the load power is step changed to 860 W, and the load current is 4.3 A. The value of the series inductance in the feedforward control has large deviation with the real value, so the output voltage drop is very large. During t_1 to t_2, the load current is greater than 1.5 A, and the parameter identification algorithm starts to be implemented. At t_2, the load power is switched to 200 W, and the load current is 1 A. The parameter identification algorithm comes to a halt. However, the value of the series inductance used in the feedforward control has reached to the real value during t_1 to t_2. At t_3, the load power is switched to 860 W. Because the value of the series inductance used in the control is close to the real value, the converter has very good dynamic response with the feedforward control. As seen in the zoom-in figure, the result is almost the same as Fig. 5(b). Fig. 8 demonstrates the effectiveness of the identification of the series inductance in DAB converter.

Fig. 9 shows the identification curve of the series inductance. At t_1, the identification method is implemented. Because there are small amounts of data at t_1, the identification result has large error. After a period of time, the series inductance becomes close to the real value.

V. Conclusion

In this letter, a parameter identification of the series inductor is proposed to improve the performance of the DAB converters. The series inductance is associated with the optimized working mode and the feedforward control. The deviation of the real value will degrade the performance of the working modes and control. The identification model of the series inductance is presented. The recursive least squares algorithm is used to get the real value of the series inductance. Finally, the experimental results show that the dynamic performance can be improved by using the parameter identification method. The uncertainty of the series inductance is removed.

References

[1] Z. Guo, K. Sun, T. Wu, and C. Li, "An improved modulation scheme of Current-fed bidirectional DC-DC converters for loss reduction," *IEEE Trans. Power Electron.*, vol. 33, no. 5, pp. 4441–4457, May 2018.

[2] Q. Tian and K. Bai, "Widen the zero-voltage-switching range and secure grid power quality for an ev charger using variableswitching-frequency single-dual-phase-shift control," *Chinese J. Elect. Eng.*, vol. 4, no. 1, pp. 11–19, Mar. 2018.

[3] N. Hou, W. Song, and M. Wu, "Minimum-Current-Stress scheme of dual active bridge DC–DC converter with unified phase-shift control," *IEEE Trans. Power Electron.*, vol. 31, no. 12, pp. 8552–8561, Dec. 2016.

[4] B. Zhao, Q. Yu, and W. Sun, "Extended-Phase-Shift control of isolated bidirectional DC–DC converter for power distribution in microgrid," *IEEE Trans. Power Electron.*, vol. 27, no. 11, pp. 4667–4680, Nov. 2012.

[5] A. Tong, L. Hang, G. Li, X. Jiang, and S. Gao, "Modeling and analysis of a dual-active-bridge-isolated bidirectional DC/DC converter to minimize RMS current with whole operating range," *IEEE Trans. Power Electron.*, vol. 33, no. 6, pp. 174–188, Jun. 2018.

[6] Z. Guo, "Modulation scheme of dual active bridge converter for seamless transitions in multiworking modes compromising ZVS and conduction loss," *IEEE Trans. Ind. Electron.*, vol. 67, no. 9, pp. 7399–7409, Sep. 2020.

[7] H. Bai, C. Mi, C. Wang, and S. Gargies, "The dynamic model and hybrid phase-shift control of a dual-active-bridge converter," in *Proc. 34th Annu. Conf. IEEE Ind. Electron.*, 2008, pp. 2840–2845.

[8] D. Segaran, D. G. Holmes, and B. P. McGrath, "Enhanced load step response for a bidirectional DC–DC converter," *IEEE Trans. Power Electron.*, vol. 32, no. 3, pp. 1964–1974, Mar. 2017.

[9] W. Song, N. Hou, and M. Wu, "Virtual direct power control scheme of dual active bridge DC–DC converters for fast dynamic response," *IEEE Trans. Power Electron.*, vol. 33, no. 2, pp. 1750–1759, Feb. 2018.

[10] N. Hou, W. Song, Y. Li, Y. Zhu, and Y. Zhu, "A comprehensive optimization control of dual-active-bridge DC–DC converters based on unified-phase-shift and power-balancing scheme," *IEEE Trans. Power Electron.*, vol. 34, no. 1, pp. 826–839, Jan. 2019.

[11] F. Xiong, J. Wu, Z. Liu, and L. Hao, "Current sensorless control for dual active bridge DC–DC converter with estimated load-current feedforward," *IEEE Trans. Power Electron.*, vol. 34, no. 1, pp. 3552–3566, Apr. 2018.

[12] Z. Shan, J. Jatskevich, H. H. Iu, and T. Fernando, "Simplified load-feedforward control design for dual-active-bridge converters with current-mode modulation," *IEEE Journal of Emerging and Selected Topics in Power Electron*, vol. 6, no. 4, pp. 2073–2085, Dec. 2018.

[13] S. Wei, Z. Zhao, K. Li, L. Yuan, and W. Wen, "Deadbeat current controller for bidirectional dual-active-bridge converter using an enhanced SPS modulation method," *IEEE Trans. Power Electron.*, vol. 36, no. 2, pp. 1274–1279, Feb. 2021.

[14] S. O. Haykin, *Adaptive Filter Theory*, 5th ed.," Englewood Cliffs, NJ, USA: Prentice-Hall, 2013.